



Title	Friction Stir Spot Welding of Pure Aluminum Sheet in View of High Temperature Deformation
Author(s)	Shibayanagi, Toshiya; Mizushima, Kenzo; Yoshikawa, Shyuhei et al.
Citation	Transactions of JWRI. 2011, 40(2), p. 1-5
Version Type	VoR
URL	<a href="https://doi.org/10.18910/11397">https://doi.org/10.18910/11397</a>
rights	
Note	

*The University of Osaka Institutional Knowledge Archive : OUKA*

<https://ir.library.osaka-u.ac.jp/>

The University of Osaka

# Friction Stir Spot Welding of Pure Aluminum Sheet in View of High Temperature Deformation<sup>†</sup>

SHIBAYANAGI Toshiya \*, MIZUSHIMA Kenzo\*\*, YOSHIKAWA Shyuhei\*\*  
IKEUCHI Kenji\*\*\*

KEY WORDS: (FSSW), (pure Al), (temperature), (flow stress), (deformation mode)

## 1. Introduction

Friction Stir Welding (FSW) and Friction Stir Spot Welding (FSSW) are now recognized as standard welding methods for aluminum alloys, and their applications have been getting diverse in many industries such as vehicles, trains, aircrafts, bridge and so on<sup>(1)</sup>. Regarding such big progress of FSW in industries, scientific approach has been also made by many researchers to reveal the secrets of FSW in terms of material flow, evolution of microstructures in the stir zone (SZ) and related metallurgical phenomena together with microstructure-dependent properties of FSW joints<sup>(2-7)</sup>.

Looking back at the history of FSW since its development by TWI, UK in 1991, the scientific approach based on "high temperature deformation" has been progressing not so significantly on remaining fundamental issues such as temperature measurement, estimation of stress level as well as strain rate which are essential for dealing with FSW in terms of deformation mechanism as proposed by M.F.Ashby et al<sup>(8)</sup>.

The deformation mode or deformation mechanism has already been investigated for some metals and ceramics such as aluminium, copper etc, and the results are well organized in "Deformation Mechanism Maps"<sup>(8)</sup> and other related papers. The map depicts each deformation mode such as creep, plastic deformation, dynamic recrystallization etc. in the coordinate system of flow stress and temperature. Thus the map helps us to investigate the heterogeneous deformation field in the stir zone of given materials during FSW and FSSW.

The temperature measurement has been successfully realized by T.H.North and his group recently giving much effective information to get a clear image of material flow and its related metallurgical aspects such as liquid film formation around the rotating tool in some magnesium alloys during FSSW<sup>(9)</sup>. The strain rate was already estimated by R.Nandan<sup>(10)</sup> and A.Gerlich<sup>(11)</sup> individually, showing us that FSW is a sort of high-strain rate deformation processing.

With these remarkable achievements in mind, further understandings of FSW is possible by putting these deformation-related data on the deformation mechanism map since the map helps us to discuss and image correctly how the material is flowing around the welding tool .

The present paper tries to measure temperature, flow stress and strain rate to define or place the deformation mode of FSSW on the deformation mechanism map of pure aluminum

## 2. Experimental

Present work utilized 99.999mass% pure aluminium sheets of 1mm thickness which was provided by Sumitomo Light Metals Co. Ltd. The aluminium sheets were cold rolled and annealed to have equi-axed grain structure with the average grain size of 140 $\mu$ m. Specimens for FSSW tests were machined from the sheet to 20mm x 20 mm with an electric discharging cutting machine. After mechanical polishing of the specimen surface, three sheets were stuck and then subjected to the welding test.

FSSW tests were performed in an ambient atmosphere with a FSW machine under the welding

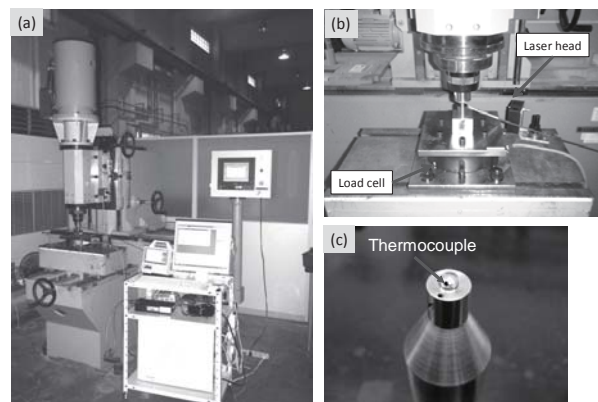


Fig.1 Experimental set-up of FSSW.

<sup>†</sup> Received on December 26, 2011

\* Associate Professor

\*\* Graduate Student

\*\*\* Professor Emeritus

conditions such as the rotation speeds of 500 and 1000RPM and the fixed dwell time of 2s. **Figure 1** shows the appearance of the present welding system (a) together with the details of welding tool and apparatus for measuring temperature, load and torque. The temperature was measured at the tip of the probe with a K-type sheath thermocouple of 0.5mm diameter, which was mounted in the welding tool as indicated in Fig.1 (c). The present system is also equipped with a load cell which measures the load along three axes and the torque around these axes individually. The specimen is mounted in a sample holder which is fixed to the rotating shaft of the welding machine, while the welding tool and measuring unit were settled on the stationary side as indicated in the figure.

Microstructural evaluation was carried out on a cross section of the welded samples with an optical microscope (OM). The sample was prepared by mechanical polishing using emery papers of the grade up to 2000 followed by electro-polishing using a mixed solution of ethanol and  $\text{HClO}_4$  with a ratio of 4:1 in volume.

### 3. Results

#### 3.1 Temperature during friction stir spot welding

**Figure 2** shows an example of temperature history during FSSW test with a rotation speed of 500RPM. The ordinate is the process time, and the abscissa is the displacement of tool and the temperature measured at the tip of the probe. As the welding tool plunges into the material, temperature raises monotonically up to around  $80^\circ\text{C}$  followed by a mild increase until 7s of the process time. Touching of shoulder to the sample surface resulted in an abrupt increase of temperature up to around  $280^\circ\text{C}$  at a process time of 11s when the plunging process completed. A steady state of temperature with a little fluctuation which might be caused by a turbulence of the thermocouple is measured during the dwelling time of 2s until the onset of tool retraction. The maximum temperature was  $289.0^\circ\text{C}$  for this case.

**Figure 3** shows an example of temperature history during FSSW test with a rotation speed of 1000RPM. As the welding tool plunges into the material, temperature rises monotonically up to around  $100^\circ\text{C}$  followed by a mild increase until 7s of the process time. Touching of shoulder to the sample surface also resulted in an abrupt increase of temperature up to around  $430^\circ\text{C}$  at a process time of 11s when the plunging process completed. A steady state of temperature with a little fluctuation is measured during the dwelling for around 2s until the onset of tool retraction. The maximum temperature was raised up to  $450^\circ\text{C}$  for this rotation speed because of the increase of frictional heat.

**Figure 4** shows the rotation speed dependence of maximum temperature during FSSW of 5N and 4N pure aluminium sheets. As is indicated in this figure, the temperature goes up almost linearly with the increase of rotation speed. The scattering of measured values is a problem of the present system. This is mainly caused by a push-back of the thermocouple since a strong force is

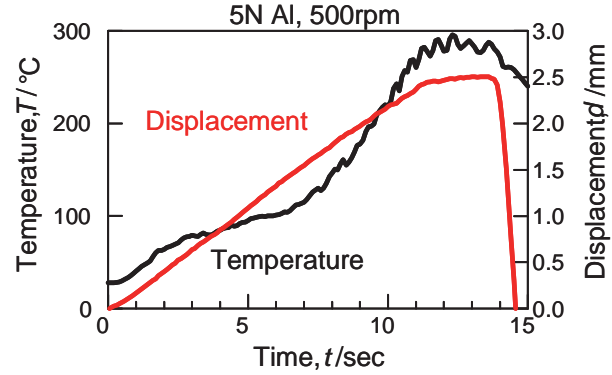


Fig.2 Temperature history during FSSW test of 5N pure aluminum sheet with a rotation speed of 500RPM.

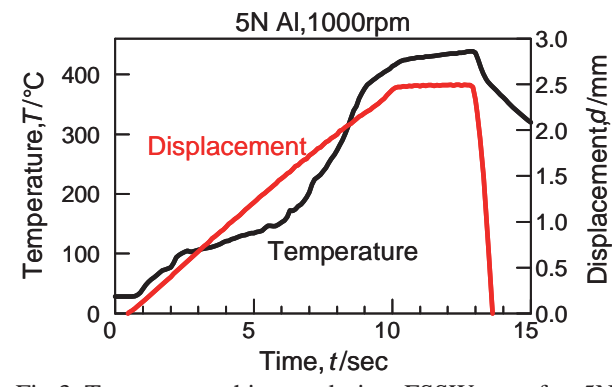


Fig.3 Temperature history during FSSW test for 5N pure aluminum sheet with a rotation speed of 1000RPM.

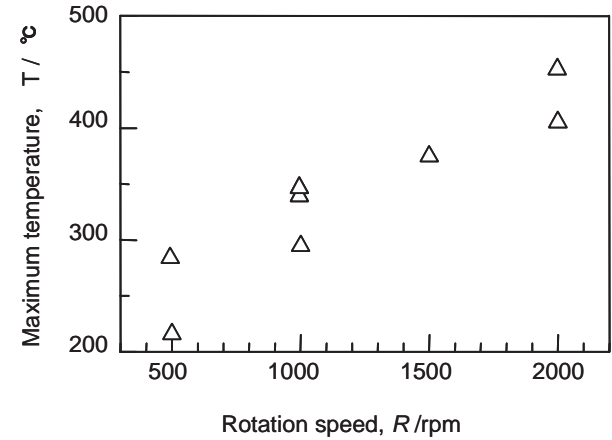


Fig.4 Rotation speed dependence of maximum temperature during FSSW of pure Al.

acting on the tip of thermocouple all the time during plunging and dwelling. Fixing the thermocouple firmly to the welding tool should be established for the sake of much more precise measurement. In any case we can measure the temperature of flowing metal during FSSW, leading us to the discussion on the deformation process of this welding method.

### 3.2 Macro and microstructure of the weld friction stir spot welded

Figure 5 shows an example of the macroscopic image of the cross section of the welded sample (a) and a close-up view of the stir zone microstructure taken from the area close to the periphery of the keyhole which is indicated by an arrow (b). Severely deformed and recrystallized regions are recognized by dark contrast in the macroscopic image. No significant growth of stir zone is observed in this welding condition, but some areas close to the probe clearly appear with the dark contrast region suggesting a peculiar microstructure such as recrystallized structure, since grain boundaries are preferentially etched.

The higher magnification revealed the detailed structure of this area, i.e. fine grain structure of equi-axed form. Since the average grain size of this area is  $1.5\mu\text{m}$  which is much smaller than that prior to the welding test, dynamic recrystallization may have occurred during welding. Concrete evidence for this phenomenon is only taken by quenching the sample just after stopping the rotating tool which is kept remained in the plate.

### 3.3 Load and torque change during FSSW

The information of flow stress during dwelling is

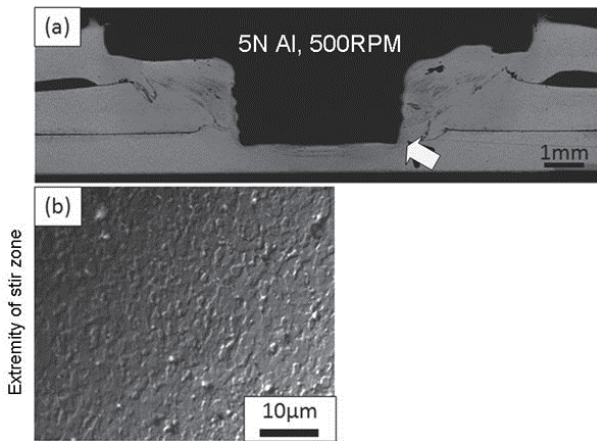


Fig.5 Microstructure on cross section of friction stir spot welded pure Al sheets

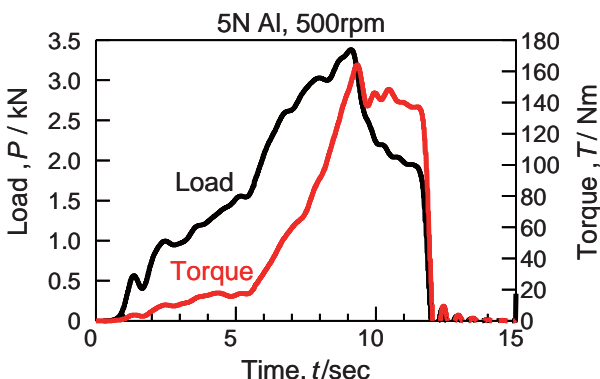


Fig.6 Changes of load and torque values during FSSW test of pure Al with a rotation speed of 500RPM.

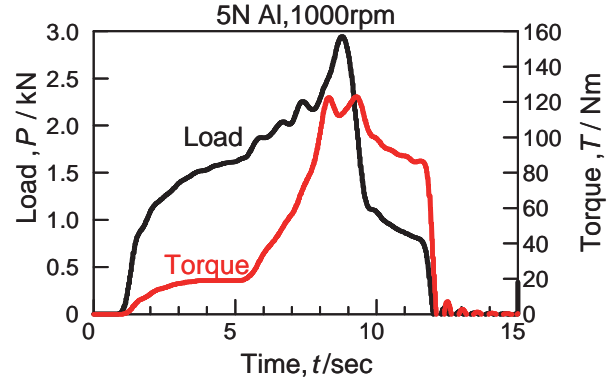


Fig.7 Changes of load and torque values during FSSW test of pure A with a rotation speed of 1000RPM.

also a key to the discussion of deformation process of FSSW and also FSW. Figure 6 shows the changes of load and torque values during FSSW test with a rotation speed of 500RPM. The ordinate represents the process time, and the abscissa represents the load and the torque values measured with the load cell equipped in the present system. Since the specimens for the present welding tests are composed of three stuck sheets, the load increases in three stages as the welding process goes on. Stage 1 is a small jump of load at the beginning of plunging which lasts for 1.8s, corresponding to the penetration of the first sheet of the specimen. Second stage is from 1.8 till 5.3s of dwell time, corresponding to the penetration of second sheet. The final stage of penetration begins at around 5.2s just after the shoulder touches the sample surface, and this last process proceeds until 9.3s when the peak value of load is recorded.

The torque value shows a steep increase after the touching of shoulder to the sample and the highest value is measured at around 9.4s, which is almost the same time as that in the load curve. Beyond this peak value the load curve shows a big drop down to 2.0kN followed by a mild decrease until 11.8s. The torque value in this stage keeps almost the same value. The dwelling period containing the peak load value represents elastic and/or plastic deformation insufficiently occurring in the material in which the temperature is not so hot as to make it yield and deform plastically. Thus the flow stress should be calculated utilizing the load value of this mild region in the load curve since no additional load is measured. The sudden drops of both load and torque values at 12s correspond to the retraction of the welding tool upon the completion of welding.

Figure 7 shows the changes of load and torque values during FSSW test with a rotation speed of 1000RPM. Both curves show similar tendency to those observed in Fig.8. The mild change of load value after the big drop from the peak value is also observed and the mean value of this region is around 0.8kN.

### 3.4 Estimation of flow stress around the welding probe

Those measured values of the load along the vertical direction lead us to the final step of the present study, *i.e.* to estimate the flow stress of the flowing metal around the rotating tool. Flow stress( $\sigma$ ) is given by the following equation (1);

$$\sigma = P/S \quad (1)$$

where,  $P$  is the load measured as explained in the previous section and  $S$  is the projected area in which the metal is flowing around the welding tool.

The projected area is uncertain at this moment since it is difficult to measure the flowing region adequately. Thus the present calculation tries to estimate both the minimum and the maximum values. The maximum flow stress is given when the region is assumed to be only one layer of the laminated material flowing just beside the probe, while the minimum value is given assuming the projected area is a summation of the area where shoulder, screw and tip of probe are contacted. The welding tool utilized is composed of a shoulder with 12mm in diameter and a probe with a M4-profile thread of which the height of screw thread is 0.38mm. Then the maximum and minimum projected area is 91.9mm<sup>2</sup> and 13.0mm<sup>2</sup>, respectively. Since the measured value of vertical load is 2.0kN the estimated flow stress is ranging from 21.8MPa to 154.7MPa for the case of 500RPM. The flow stress for 1000RPM case is calculated in the same way and the value is ranging from 10.8MPa to 61.8MPa.

#### 4 Discussions

##### 4.1 Deformation modes in FSSW and FSW

Friction related welding processes are accompanied by peculiar plastic deformation modes which are unique for each welding method. For example friction welding employs compression and torsion, ultrasonic vibration welding is based on a mixture of compression and shear deformation. FSW is thought to mainly progress by a shear deformation since it is straightforward to imagine the interface between the rotating stir zone and its contacting base metal called TMAZ, and indeed some texture analyses on friction stir welded metals revealed shear-texture in the stir zone<sup>(12, 13)</sup>.

However with some proposed metal flow models in mind, it should be noticed that single mode of deformation cannot be applied to explain the entire process of FSW and FSSW. Flow of metal in the region contacting the shoulder should be different from that around the probe, and yet different from that inside the stir zone or the extremity of the stir zone surrounded by base metal which is in stationary state. In fact compression mode is found by a texture analysis of single crystal pure aluminium, and this plastic deformation is caused by the growth of stir zone<sup>(14)</sup>. And also the flow behaviour alters depending on the location through the thickness of material being welded. It is also found that FSSW possessed grain boundary sliding in the SZ of 2024-T3 aluminum alloy<sup>(15)</sup>, suggesting superplastic deformation is another part of deformation apart from the dynamic recrystallization phenomenon in the stir zone.

Therefore deformation in FSSW needs to have a

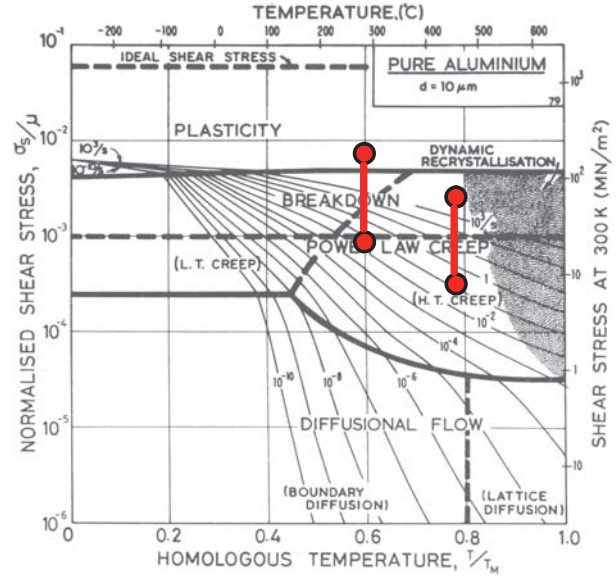


Fig. 8 Present data imposed on the Deformation mechanism map of Al.

concept of “multi-mode” for the sake of precise description, and the concrete image will be given by investigating each area of FSSW joints in view of temperature, flow stress, strain rate etc, likewise that commonly regarded as targets of investigation in the science of high temperature deformation.

##### 4.2 Comparison with deformation mechanism map of pure aluminum

As discussed in the previous section different deformation modes may proceed simultaneously during FSSW. Among such diversity the present study focused on the region close to the probe since the present system measures the temperature at the tip of probe.

**Figure 8** shows the present data imposed on the deformation mechanisms map of pure aluminium<sup>(8)</sup>. The ordinate represents flow stress normalized by the stiffness of pure aluminium such as 26GPa. The abscissa is homologous temperature. This map consists of some regions called Power-Law Creep regions (High-Temperature and Low-Temperature), diffusional flow such as boundary diffusion and lattice diffusion, where each border is drawn by calculating the equilibrium of constitution equations of the neighbouring deformation mechanisms. Re-examination of this map has been conducted and a revised map is given by Sato et al.

Present data on this map mean that the metal flow around the probe is recognized as a plastic deformation accompanying dynamic recrystallization process. However the lowest value of those plots is in the region of power law creep. This implies that the other deformation mechanism is dominantly proceeding in the stir zone or other region where metal flows with much lower flow stress. In fact superplastic deformation is pointed out to take place in the stir zone of A2024 aluminum alloy during friction stir spot welding. Thus

FSSW and FSW may occur by different deformation modes simultaneously depending on the location around the tool, and this heterogeneity of deformation modes is the essence of these novel joining techniques.

## 5. Summary

Temperature at the tip of probe, vertical load and torque around the vertical axis were measured during FSSW of high-purity aluminum sheets. The measured values were utilized to estimate flow stress. Maximum temperatures decreased from 450°C to 289°C in accordance with the reduction of rotation speed from 1000RPM to 500RPM. The estimated flow stress of the flowing metal around the probe ranged from 154.7 to 21.8MPa at a rotation speed of 500RPM, and from 10.8MPa to 61.8MPa at 1000RPM. These values were in the dynamic recrystallization region of the Deformation Mechanism Map, but the map also suggests that some other deformation mechanism possibly proceeds during FSSW. Analyses of flow stress and also strain rate is a strong tool for us to get more detailed feature of FSSW.

## 5. Acknowledgement

One of the authors (T.S.) wishes to thank The Light Metal Educational Foundation Inc. for financial support. The present paper was originally published from the proceedings of Int'l Conf. on Metallography 2010, High-Tatras, Slovakia (2010), 59-67.

## Reference

- [1] R.S.Mishra and Z.Y.Ma: Metall. Mater. Sci. Eng., **R50** (2005), 1-78.
- [2] A.P. Reynolds: Scripta Mater., **58**(2008), 338-342.
- [3] S.Muthukumaran and S.K.Mukherjee: Science and Technology of Welding & Joining, **11**(2006), 337-340.
- [4] W.J. Arbegast: Scripta Mater., **58**(2008), 372-376.
- [5] M.Fujimoto et al.: Science and Technology of Welding & Joining, **13**(2008), 663-670.
- [6] G.M. Xie et al.: Mater. Sci. Eng., **471**(2007), 63-68.
- [7] M.Yamamoto et al: Sci. Tech. Welding and Joining, **13**(2008), 583-592.
- [8] M.F.Ashby: Acta metal., 20(1972), 887-897.
- [9] T.H. North, G.J. Bendzsak, C.B. Smith, and G.H. Luan: Proc. 7<sup>th</sup> Int. Symp. Kobe, Japan, 2001, JWS, Tokyo, pp. 621-32.
- [10] R. Nandan, G.G. Roy, and T. DebRoy: Metall. Mater. Trans. A, 2006, vol. 37A, pp. 1247-59.
- [11] A.Gerlich, M.Yamamoto and T.H.North: Metall. Mater. Trans. A, **38A**(2007), 1291-1302.
- [12] J.A. Schneider and A.C. Nunes: Metall. Mater. Trans. B, **35B**(2004), 777-83.
- [13] R.W. Fonda and J.F. Bingert: Metall. Trans. **35A**(2004), 1478-99
- [14] T.Shibayanagi et al: Metall. Mater. Trans. **40A** (2009), 920-931.
- [15] A.Gerlich and T.Shibayanagi: Scripta Mater. **60**(2009), 236-239.